

## EQUATIONS OF STATE IN SOIL COMPRESSION BASED ON STATISTICAL MECHANICS

MASAHARU FUKUE<sup>i)</sup> and CATHERINE N. MULLIGAN<sup>ii)</sup>

### ABSTRACT

There have been many theories and interpretations of the compression process for soil. However due to the complexity of the compression process for a wide range of soil states, i.e., suspended, liquid, plastic, semisolid or solid states like rock, the interaction between the states or the transition from one state to another, there have often been misunderstandings and difficulties regarding the application of these theories. In this study, an ideal particle distribution in an ideal ground system is derived to find the equation of state, a general compression process for a wide variety of soil types and states. In other words, it is a general relationship between the void ratio and effective overburden pressure in terms of interparticle energy and is thus a “law of soil.” The principle is based on the law of energy distribution in statistical mechanics. The derived equations can be applied to describe the void ratio profile and the compression process of various soils. Case studies show that this theoretical approach agrees well with the experimental data obtained for several soils such as sediments, Mexican City clay, sand and others.

**Key words:** compression, interparticle energy, law of soil, particle distribution, void ratio (IGC: D5)

### INTRODUCTION

The process of soil consolidation in nature takes place over a period of many thousands of years. This process can be expressed in terms of volume, pressure and energy state, i.e., interparticle energy. Difficulties within soil mechanics exist because of the varied nature of the soil state in terms of interparticle energy, and because there are no “equations of state” for soil materials. This is mainly because of the compressible and irreversible nature of the interactions of soil particles.

The first impression is that the void ratio ( $e$ ) profile in the soil is determined by the overburden pressure ( $p$ ). However, this pressure is also controlled by the fabric of the soils, which can be related to the void ratio. Therefore, many studies have been carried out to describe and express the  $e$ - $\log p$  relationship for soils (Skempton, 1944; Nishida, 1959; Oswald, 1980; Fukue and Okusa, 1987). Because this relationship can provide the state for soils in terms of volume (volume ratio or void ratio) and pressure (usually effective overburden pressure), it could be used to describe the shear strength characteristics (Schofield and Wroth, 1968; Leroueil and Vaughan, 1990; Burland, 1990). Nevertheless, the relationships between volume and pressure obtained have been always empirical, and consequently the interpretations have been made based on empirical relationships. This has provided many theories and interpretations for the compression process and compression index of soils from different

view points (Yoon et al., 2004; Park et al., 2004; Giasi et al., 2003; Tsuchida, 2001; Burland, 1990; Butterfield, 1979). However, at present, due to its complexity, there may be some misunderstandings for the compression of soils.

It is known that the state of fine soils changes in terms of water content. The boundaries have been provided by the liquid, plastic and shrinkage limits. This concept can be extended from the suspended state (Imai, 1980; Imai, 1981; Been and Sill, 1981) to sedimentary rock. Thus, soil particles with the entire soil system are varied in their nature, from suspended, to deposited, consolidated and cemented states, though the boundaries are not often clear. For example, the definition of the bottom surface under marine conditions has not been established yet, because it is difficult to describe the general aspect of the boundary between suspended and deposited states there. Fukue et al. (1987) found that there is a very loose sediment layer on the top of the sea bottom from sedimentation experiments and field observations. Since the void ratio of this layer decreases abruptly with depth, its characterization is often difficult. Fukue et al. (1987) used a concept of average void ratio to characterize this thin top layer and found that the void ratio decreases to half of the surface void ratio at a depth of about 5 cm. Thus, this layer has different characteristics from the suspended solid systems or sediments, possibly according to the types of interactions. Herein, suspended solid systems consist of solid particles without contact and interacting

<sup>i)</sup> Department of Marine Civil Engineering, Tokai University, Shizuoka, Japan (fukue@scc.u-tokai.ac.jp).

<sup>ii)</sup> Department of Building, Civil and Environmental Engineering, Concordia University, Montreal, Quebec, Canada.

The manuscript for this paper was received for review on May 9, 2008; approved on November 27, 2008.

Written discussions on this paper should be submitted before September 1, 2009 to the Japanese Geotechnical Society, 4-38-2, Sengoku, Bunkyo-ku, Tokyo 112-0011, Japan. Upon request the closing date may be extended one month.

only by repulsive forces such as dispersed montmorillonite clay particles in distilled water, while sediments exhibit an ordinary structure similar to soil. Furthermore, it was found that the void ratio of the top layers of sediments (about 5 cm) can be given by a simple empirical formula using the average void ratio system of sediments (Fukue and Okusa, 1987; Fukue et al., 1987).

In this study, the empirical formula, an average void ratio–depth relationship obtained previously, is shown to be derived theoretically from statistical mechanics and can be applied to other states of soils, such as suspended soils, ordinary plastic soils, peat, sand, etc. However, its application shows that the compression curve,  $e$ - $\log p$  curve, will not have a straight portion (Fukue and Okusa, 1987), although it seems to be so, and that the compression curve through the boundaries from one to another state would be irregular (Imai, 1980; Imai, 1981). Thus, the phenomena observed experimentally have often confused engineers and researchers. Since soil is a compressible and irreversible material, it is quite difficult to treat it thermodynamically. This is because the compression process produces dissipation energy, and unknown variables such as entropy have to be introduced. This may be one of the reasons why the state equation of soil has not been developed.

In this study, soil systems consisting of elements with different void ratios are considered. Considering that each element is subjected to the corresponding overburden pressure, the system can be converted to the compression process, as illustrated in Fig. 1. The advantage in utilizing the soil system instead of a process is to minimize the number of unknown variables.

Characterizing the overburden pressure to void ratio, the relationship ( $e$ - $\log p$ ) between the void ratio and the effective overburden pressure becomes unique. This is why the void ratio–pressure relationships for various soils such as sands and clays are similar. This also indicates that there is a “law of soil” that exists in a similar way to the “law of atmosphere” established in statistical mechanics (Reif, 1965).

In this study, an ideal particle distribution is used to derive a general compression process. Void ratio (volume), pressure and energy terms are taken into con-

sideration. Since the equation of state is the most basic volume–pressure relationship for substances, to describe the state during compression, as is well known for ideal gases, the development of a relationship makes it easier for soils to be treated in a more scientific manner. Case studies are also used to illustrate the applicability of this approach.

## BACKGROUND

Geotechnical engineering has often been based on the testing of sampled soils. The basic concept is that the reloading for sampled soil will return it to the in-situ condition, because it is assumed that the compression index,  $C_c$  is constant for the original and reloaded soil, as illustrated in Fig. 2. This concept has been widely accepted and used for the prediction of settlement and the concept of shear strength, though further modifications have been made using reconstituted soils which can provide a standard compression line, such as an intrinsic compression line (ICL) and a sedimentation compression line (SCL) for shallow marine deposits (Butterfield, 1979; Leroueil and Vaughan, 1990; Burland, 1990). The ICL and SCL may correspond to compression for remoulded soils and natural compression lines, respectively. This is also an important subject in this study and will be discussed later.

On the other hand, the empirical facts have shown that the samples taken from different depths have different values of  $C_c$ , as illustrated in Fig. 3(a) and (b). As a result, the compression index becomes a function of the initial void ratio prior to the loading for testing. Many references such as Nishida (1959) and Oswald (1980) have shown that this relationship is close to linear as known empirically. If the empirical relationships are correct, there might be an inconsistency between Figs. 2 and 3.

Researchers and engineers who realized this inconsistency have thought that the inconsistency resulted from the disturbance of the samples (Mesri et al., 1975; LaRochelle et al., 1980; Leroueil and Vaughan, 1990). Therefore, relatively low values of  $C_c$  have been obtained for the disturbed samples. It is true that for highly cemented or sensitive soils, the value of  $C_c$  will decrease

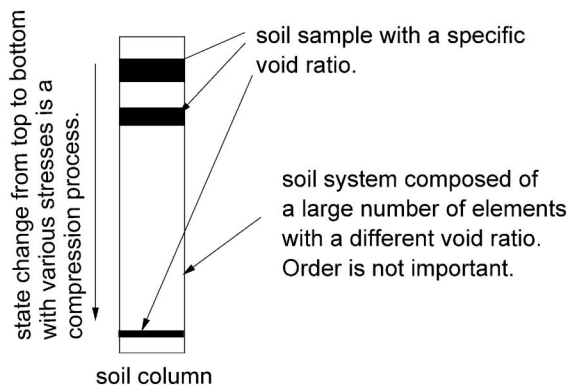


Fig. 1. Concept of process and system in a soil column

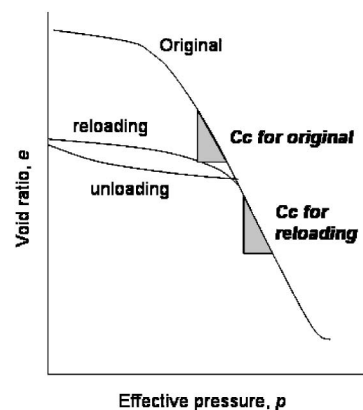


Fig. 2. Illustration of a general  $e$ - $\log p$  relationship in soil compression

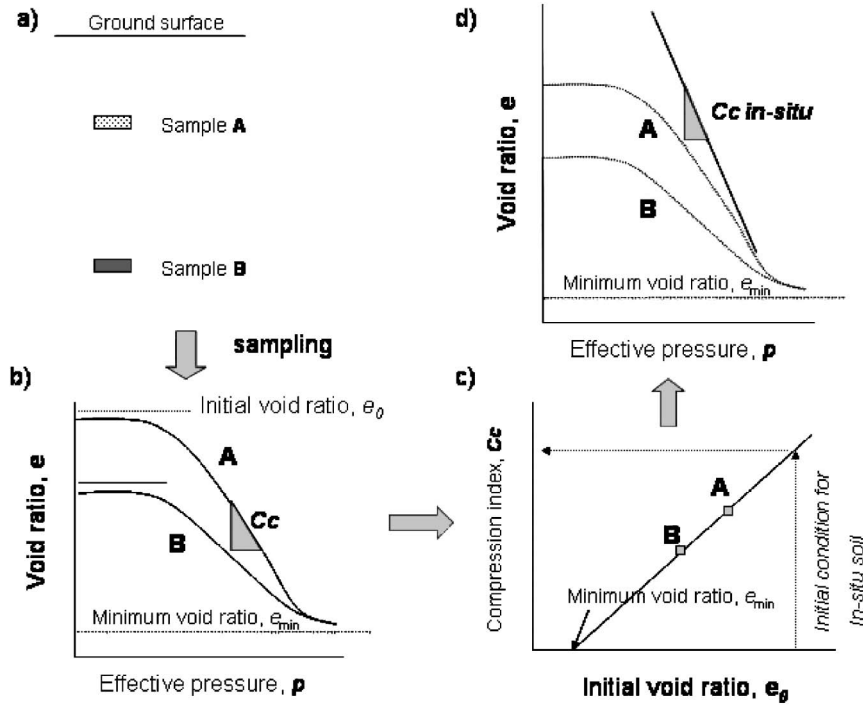


Fig. 3. Hypothetical compression behaviour of sampled soils after stress release and prediction of natural compression

with disturbance. This can be explained by strain softening during compression, as explained in later sections. However, the dependency of the initial void ratio on  $C_c$  is not due to the disturbance of the sample, but is an inherent property of soils. This will be discussed in this paper.

It has been shown that there is a good relationship between  $C_c$  and the initial void ratio adjusted to the water content of the liquid limit (Burland, 1990). In this case, it can be emphasized that  $C_c$  will vary as if the relationship is a function of soil type. However, if  $C_c$  is dependent on the initial void ratio alone, then the influence of soil type will vanish. This becomes clear by the existence of a universal formula representing the  $e$ - $\log p$  relationship for varied states and types of soils. The above-mentioned is very important not only for prediction of soil properties and behaviour including settlement and shear strength, but also for the fundamentals in soil mechanics and geotechnical engineering.

The authors consider that the present situation may result from a lack of theoretical examination based on the empirical data. As mentioned earlier, the application of thermodynamics is not practical, because of many unknown factors. Statistical mechanics can be easier to apply for a soil system for many reasons, as shown throughout this paper.

### FUNDAMENTAL RELATIONSHIP BETWEEN PRESSURE, VOLUME AND POTENTIAL ENERGY

The conventional relationship in geotechnical engineering for void ratio and pressure is often given in the following form:

$$p = \frac{\gamma_s z}{1 + e} \quad (1)$$

Where  $p$  is the effective overburden pressure,  $e$  is the void ratio,  $\gamma_s$  is the submerged unit weight of the solid and  $z$  is the soil depth under consideration. In Eq. (1), a critical assumption is that the void ratio is constant over depth. Therefore, this will not be applied to the variable void ratio  $e$ .

Therefore, a generalized relationship between effective pressure and void ratio can be expressed as:

$$p(z) = \frac{\gamma_s z}{1 + \bar{e}(z)} \quad (2)$$

where  $p(z)$  is the overburden pressure as a function of the depth  $z$ , and  $\bar{e}(z)$  is not constant, but variable with the profile of the average void ratio of a soil column with depth  $z$ , as shown in Fig. 4. In Fig. 4, the difference between average void ratio and true void ratio with depth  $z$  is clear. Thus, the profile of the overburden pressure is independent of the true void ratio, but is directly dependent on the average void ratio profile. If the profile of  $\bar{e}$  is determined, then the profile of  $p$  can be obtained when the  $e$ - $p$  or  $e$ - $\log p$  relationship is derived from the  $e$  and  $\bar{e}$  relationship (Fukue and Okusa, 1987).

$$\bar{e}(z) = \frac{\int e(z) dz}{z} \quad (3)$$

Equation (2) can be rewritten as  $p(z) (1 + \bar{e}(z)) = mgz / V_s$ , where  $V_s$  is the volume of the solid portion of the soil and can be assumed to be unity, because the unity in the term  $(1 + \bar{e}(z))$  resulted from the assumption that the volume of

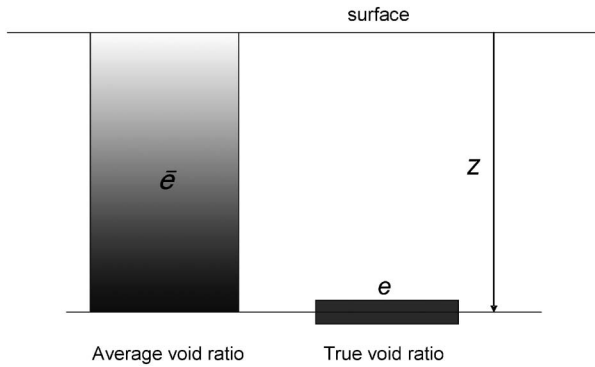


Fig. 4. Definition of average void ratio when the true void ratio varies with depth

the solid portion is unity. Therefore, the term  $(1 + \bar{e}(z))$  provides the volume of a soil element and  $mgz$  is proportional to the potential energy of the soils having a volume of  $1 + \bar{e}(z)$ . Although one may think that  $mgz$  is the potential energy, this is not the case because  $z$  does not indicate the depth or height of the center of gravity. This will be discussed in a later section.

The relationship can be represented by Eq. (2)'

$$p(z)V(z) = mgz \quad (2)'$$

or more simply as,

$$pV = E'_p \quad (2)''$$

Where  $E'_p = mgz$ . This is proportional to the potential energy of the soil element. Equation (2)'' suggests that the characteristics of the soil volume change can be expressed by  $pV = \text{variable}$ , and can be compared to the equation of state for an ideal gas, i.e.,  $pV = \text{constant}$ , in which the molecules have no interaction. In fact, this comparison is not essential, because the former deals with a soil system and the latter describes an ideal gas element. However, even if a soil element was used, the relationship for a soil element can be more complicated due to the existence of the interactions between particles. Thus, the difference between the two substances may be due to the interaction between particles for soil or gas molecules. If the description here is true, Eq. (2) would be the most fundamental and substantial expression, i.e., the state equation of soil. This is one of the most important aspects in this study and this will be established through this study. Therefore, one of the objectives of this study is to examine Eq. (2)' or Eq. (2)'' to establish the  $\bar{e}(z)$  formula as an equation of state for soil.

## ENERGY DISTRIBUTION

Theoretical development in this study is based on statistical mechanics which may not be familiar to most readers. Therefore, it seems that the derivation of equations is a little complicated, as shown in Fig. 5.

The first problem is to derive the most probable potential energy distribution of particles. This is achieved by using a constant total potential energy with elevation and

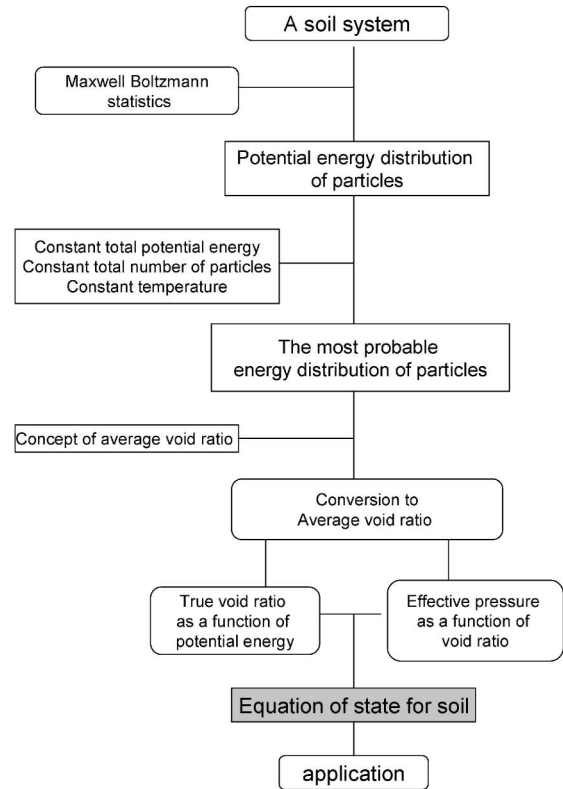


Fig. 5. Flowchart of the theoretical development in this study

the total number of particles. In this formulation, the interparticle energy is included in the potential energy by changing the mass of the particles. It will appear in the parameter based on the experimental results.

The next step is to transform the number of particles to void ratio. The concept of average void ratio system is conveniently used in this conversion. The average void ratio system is also theoretically converted into the true void ratio system. These void ratios are expressed as a function of potential energy which is also a function of depth if it is needed to use. The effective pressure is expressed as a function of the void ratio. Thus, the relationship between pressure, volume and potential energy is obtained.

### Probability of Particle Distribution

Consider a system with a large number of particles  $n$  and that the particles are enclosed in a large number of immobile containers as shown in Fig. 6. The first container at the bottom contains  $n_1$  number of particles at an energy level of  $\varepsilon_1$ . The next level has  $n_2$  particles at an energy level of  $\varepsilon_2$  and so on. Since the total number of particles is  $n$ , the number of possible distributions,  $\Omega$ , based on Maxwell-Boltzmann statistics, is given by:

$$\Omega = n! / n_1! n_2! n_3! \dots n_r! \dots \quad (4)$$

Now, the most probable distribution with a constant total energy  $E$  can be obtained at the maximum value of  $\Omega$ . If one particle is moved from the second container to the third container and if another particle is moved from the

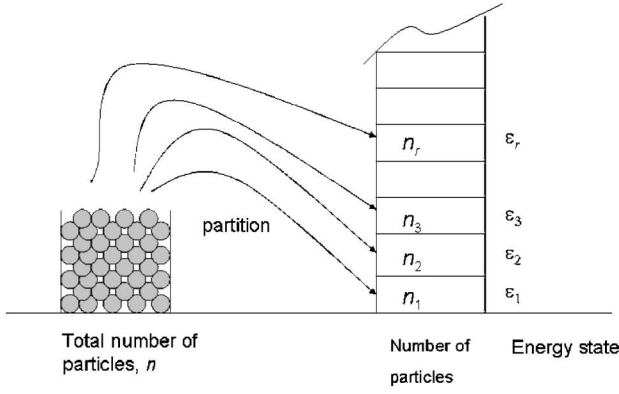


Fig. 6. Particle distribution into piled boxes

second to the bottom container, the new distribution is given by:

$$\Omega' = n! / (n_1 + 1)! (n_2 - 2)! (n_3 + 1)! n_4! \dots n_r! \dots \quad (5)$$

The ratio of Eq. (5) to Eq. (4) is then:

$$\begin{aligned} \Omega' / \Omega &= \frac{n! / n_1! n_2! n_3! \dots n_r!}{(n_1 + 1)! (n_2 - 2)! (n_3 + 1)! n_4! \dots n_r!} \\ &= \frac{n_2(n_2 - 1)}{(n_1 + 1)(n_3 + 1)} \end{aligned} \quad (6)$$

Then if  $n_1$ ,  $n_2$  and  $n_3$  are very large numbers, Eq. (6) becomes:

$$\Omega' / \Omega = \frac{(n_2)^2}{n_1 n_3} \quad (7)$$

Since there is no change in energy in the system, then the ratio  $\Omega' / \Omega$  in Eq. (7) must be equal to 1 and then the steady state of the system can be obtained as:

$$n_1 / n_2 = n_2 / n_3 \quad (8)$$

Including the other particles will give the following relationship:

$$n_1 / n_2 = n_2 / n_3 = n_3 / n_4 = n_4 / n_5 = \dots = n_i / n_j = n_j / n_k \dots \quad (9)$$

This leads directly to:

$$n_2 = n_1 \exp(-\mu \varepsilon_1), \quad n_3 = n_1 \exp(-\mu \varepsilon_3),$$

Therefore, the most appropriate profile can be given by Eq. (10) and is illustrated in Fig. 7:

$$n_r = n_1 \exp(-\mu \varepsilon_r) \quad (10)$$

where  $\varepsilon_r$  ( $r = 1, 2, 3 \dots r \dots$ ) is the energy state corresponding to  $n_r$  and  $\mu$  is a physical constant to be discussed later.

#### Partition Function

The Stirling approximation for a large  $n$  for Eq. (4) can be expressed as:

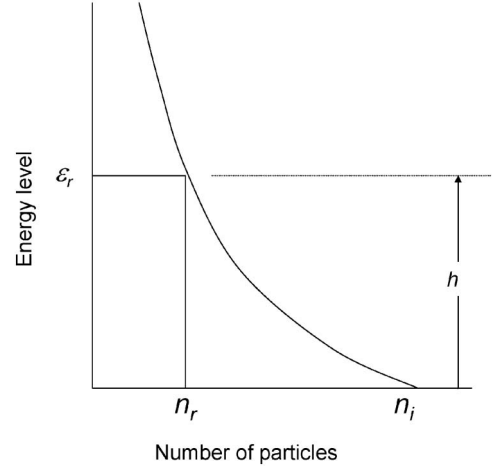


Fig. 7. Probable distribution of particles

$$\begin{aligned} \ln \Omega &= \ln(n!) - \sum \ln(n_r!) \\ &= \ln(n!) - \sum (n_r \ln n_r - n_r) \\ &= \ln(n!) - \sum n_r \ln n_r + \sum n_r \end{aligned} \quad (11)$$

If an increment of  $\ln \Omega$  is taken, and  $n!$  and  $\sum n_r$  can be assumed to be constants, then:

$$\begin{aligned} \delta \ln \Omega &= 0 - \sum \{ \delta n_r \ln n_r + (n_r / n_r) \delta n_r \} + 0 \\ &= - \sum \{ (\ln n_r + 1) \delta n_r \} \end{aligned} \quad (12)$$

If no energy is added, then Eq. (12) is equal to 0 (Tolman, 1979). If a number of particles ( $\delta n_r$ ) are added to a group of particles with an energy level of  $\varepsilon_r$ , then the energy level of that group changes from  $n_r \varepsilon_r$  to  $(n_r + \delta n_r) \varepsilon_r$ . If it is assumed that the total energy is constant, then :

$$\delta E = \sum \varepsilon_r \delta n_r = 0 \quad (13)$$

where  $E$  is the total energy.

If the total number of particles is constant, then:

$$\sum \delta n_r = 0 \quad (14)$$

To maximize  $\Omega$  in Eq. (12), the following equation is required:

$$\sum \ln n_r \delta n_r = 0 \quad (15)$$

Equations (13), (14), and (15) do not include the total number of particles and the total energy  $E$ . To relate these equations then to these parameters, two constants must be introduced, the dimensionless  $\lambda$  and  $\mu$  which is a reciprocal of the energy term. Multiplying Eq. (13) by  $\mu$  gives:

$$\sum \mu \varepsilon_r \delta n_r = 0 \quad (16)$$

Similarly, multiplying Eq. (14) by  $\lambda$  leads to:

$$\sum \lambda \delta n_r = 0 \quad (17)$$

Adding Eqs. (15), (16) and (17) gives:

$$\sum (\ln n_r + \lambda + \mu \varepsilon_r) \delta n_r = 0 \quad (18)$$

or

$$\ln n_r + \lambda + \mu \varepsilon_r = 0 \quad (19)$$

Rearranging Eq. (19), gives:

$$n_r = \exp(-\lambda) \exp(-\mu \varepsilon_r) \quad (20)$$

where the total number of particles is

$$\begin{aligned} n &= n_1 + n_2 + n_3 + \dots + n_r + \dots \\ &= \exp(-\lambda) \{ \exp(-\mu \varepsilon_1) + \exp(-\mu \varepsilon_2) + \dots \} \\ n &= \exp(-\lambda) \sum \exp(-\mu \varepsilon_r) \end{aligned} \quad (21)$$

Then,

$$\exp(-\lambda) = n / \sum \exp(-\mu \varepsilon_r) \quad (22)$$

By substituting Eq. (22) into Eq. (20), the following fundamental equation used in statistical mechanics (Reif, 1965) is obtained:

$$n_r = \frac{n \exp(-\mu \varepsilon_r)}{\sum \exp(-\mu \varepsilon_r)} \quad (23)$$

$$n_r = \frac{n \exp(-\mu \varepsilon_r)}{P} \quad (24)$$

where,

$$P = \sum \exp(-\mu \varepsilon_r) \quad (25)$$

which is the partition function for the energy system.

#### Physical Meaning of $\mu$

The change in internal energy of a substance resulting from a volume change is thermodynamically expressed by

$$\delta E = T \delta S - p \delta V \quad (26)$$

where  $E$  is the internal energy,  $T$  is the absolute temperature,  $S$  is the entropy,  $p$  is the pressure and  $V$  is the volume.  $S$  is defined by:

$$S = k \ln \Omega \quad (27)$$

where  $k$  is the Boltzmann constant. From the microscopic point of view, the internal energy equals  $\sum \varepsilon_r n_r$ . Therefore, the change in internal energy is given as:

$$\delta E = \sum \varepsilon_r \delta n_r + \sum n_r \delta \varepsilon_r \quad (28)$$

A Comparison of Eqs. (13) and (28) indicates that the second term on the right hand side of Eq. (28) is due to a volume change, because the number of particles remains constant. Therefore, the first term of the right side of Eq. (26) corresponds to the first term of Eq. (28). Thus the

following equation is obtained:

$$T \delta S = \sum \varepsilon_r \delta n_r \quad (29)$$

On the otherhand, from Eqs. (27), (12) and (20), the left side of Eq. (29) is then:

$$\begin{aligned} T \delta S &= T(k \delta \ln \Omega) \\ &= kT \left( - \sum \ln n_r \delta n_r \right) \\ &= kT \left[ - \sum \ln \{ \exp(-\lambda) \exp(-\mu \varepsilon_r) \} \delta n_r \right] \\ &= kT \left[ - \sum \{ -\lambda - \mu \varepsilon_r \} \delta n_r \right] \end{aligned} \quad (30)$$

From Eqs. (17) and (30), then

$$T \delta S = kT \mu \sum \varepsilon_r \delta n_r \quad (31)$$

From Eqs. (29) and (31), the following important relationship is obtained:

$$\mu = 1/\kappa T \quad (32)$$

If this is substituted into Eq. (24), then the result is the well known energy distribution of Maxwell-Boltzmann:

$$n_r = \frac{n \exp(-\varepsilon_r/kT)}{P} \quad (33)$$

where  $n_r$  is the number of particles at an energy level of  $\varepsilon_r$ .

#### Particle Distribution

For a given soil system, the partitioning function,  $P$  expressed by Eq. (25) is a constant value. Therefore, the distribution of particles given by Eq. (33) is governed by the energy level,  $\varepsilon$ , where  $n$ ,  $k$  and  $T$  are regarded as constants.

If a particle exists at height  $h$  from ground level, as shown in Fig. 7, and assuming that there are no interparticular forces acting between the particles, the potential energy is then  $mgh$ , where  $m$  is the mass of the particle and  $g$  is the gravitational acceleration. However, the assumption above cannot be valid, since there are particle interactions. By using the concept of imaginary particles, as described later, this can be corrected. At a potential energy level of  $\varepsilon_r$ , the number of particles in a soil volume with a unit area and thickness of  $\delta h$  is expressed as:

$$n_r(h) \delta h = \frac{n \exp(-mgh/kT) \delta h}{P} \quad (34)$$

Using the  $h$ - $z$  relationship where  $h = (z_c - z)$  as shown in Fig. 8, then Eq. (34) becomes:

$$n_r(z) \delta z = \frac{n \exp(-mg(z_c - z)/kT) \delta z}{P} \quad (35)$$

where  $z_c$  is the total height or thickness of the soil ground system, which can represent the "size of the system."

## DISTRIBUTION OF VOID RATIO

### Average Void Ratio System

For a system with equi-dimensional particles of volume,  $V_p$ , for each particle, then the average void ratio in a soil column (Fig. 4) which has a unit area  $A$  and thickness of  $z$ , is expressed as:

$$\bar{e}(z) = \frac{V_v}{V_s} = \frac{Az - V_s}{V_s} \quad (36)$$

where  $V_s$  and  $V_v$  are the volumes of the solid and pore spaces, respectively. Expressing the number of particles in the soil column by  $N$ , then:

$$V_s = NV_p \quad (37)$$

From Eqs. (36) and (37),

$$\bar{e}(z) = \frac{Az}{NV_p} - 1 \quad (38)$$

where  $z > 0$ . If  $z$  is taken between 0 and  $z_c$  for a given soil system as shown in Fig. 8, then  $\bar{e}$  will vary from a particular value at the surface to the average void ratio for the entire soil system. The two extreme void ratios at  $z=0$  and  $z=z_c$ , then will be used as the boundary conditions to obtain a relationship between the average void ratio and the energy term.

### Average Void Ratios as Boundary Conditions

The void ratio  $e_0$  in which  $z$  is very small ( $\delta z$ ) is dependent on the soil structure. The value is assumed to be an arbitrary constant and herein accords with the surface void ratio, as shown in Fig. 8. However, in this study,  $e_0$  can be defined for any initial void ratio prior to loading. The void ratio of a soil column whose thickness varies with  $z$  is defined as the average void ratio of the system  $\bar{e}$ . As far as the void ratio decreases down to the  $e_{\min}$  at  $z=z_c$ , the void ratio of the total column ( $e_c$ ) will be the minimum average void ratio, as shown in Fig. 8, and is thus defined as the minimum average void ratio.

a) Surface void ratio,  $e_0$

The void ratio of a very thin surface soil layer, with thickness of  $z_0 (= \delta z)$  is defined as the surface void ratio. Expressing the number of particles as  $N_0$ , the surface void ratio is defined as:

$$e_0 = \frac{Az_0}{N_0 V_p} - 1 \quad (39)$$

b) Minimum average void ratio,  $e_c$

$$e_c = \frac{Az_c}{N_c V_p} - 1 \quad (40)$$

where  $N_c$  is the total number of particles at this void ratio.

### Relationship between Void Ratio and Potential Energy

a) Average void ratio system

The size of the system with an average void ratio is given by the range from  $e_0$  to  $e_c$  which is defined as the minimum average void ratio and equals the average void ratio of a total soil system. For a soil state with an ar-

bitrary void ratio at depth  $z$ , a function  $F'_r$  is defined as:

$$F'_r = \frac{\bar{e}(z) - e_c}{e_0 - e_c} \quad (41)$$

Substituting Eqs. (38) to (40) into Eq. (41), gives the following:

$$F'_r = \frac{N_0(N_c z - N_c z_c)}{N(N_c z_0 - N_0 z_c)} \quad (42)$$

To derive  $F_r$  in terms of potential energy, the distribution of particles given by Eq. (35) can be used. For example, the number of particles in a column of thickness  $z$  can be expressed in two ways, i.e., by integrating Eq. (35) over depth and by using the average number of particles at the center of gravity of the column as shown in Fig. 9. The integration gives:

$$\begin{aligned} N &= Cn \int_{z_c - z}^{z_c} \exp \{(-mgh)/kT\} dh \\ &= Cn(kT/mg) [\exp \{-mg(z_c - z)/kT\} \\ &\quad - \exp \{mgz_c/kT\}] \end{aligned} \quad (43)$$

where  $C$  is a constant which equals the reciprocal value of the partition function. It is noted that the partition function  $P$  expressed by Eq. (25) is obviously constant for a given soil energy system.

Using the average number of particles, the number of particles contained in the column with a depth of  $z$  is given by:

$$\begin{aligned} N &= \bar{n}z \\ &= Cnz \exp \{-mg(z_c - z_G)/kT\} \end{aligned} \quad (44)$$

where  $z_G$  is the depth at the center of gravity of the column with depth of  $z$  and  $\bar{n}$  is the average number of particles over the depth  $z$ .

From Eqs. (43) and (44),  $z$  can be expressed then as:

$$z = \frac{kT/mg [\exp \{-mg(z_c - z)/kT\} - \exp \{mgz_c/kT\}]}{\exp \{-mg(z_c - z_G)/kT\}} \quad (45)$$

Similarly,  $N_0$ ,  $N_c$ ,  $z_0$  and  $z_c$  are also expressed in two ways. By integrating Eq. (35) over depth, from  $z=0$  to  $z=z_0$ ,  $N_0$  can be expressed as:

$$\begin{aligned} N_0 &= Cn(kT/mg) [\exp \{-mg(z_c - z_0)/kT\} \\ &\quad - \exp \{mgz_0/kT\}] \end{aligned} \quad (46)$$

In terms of the average number of particles, the equation is:

$$N_0 = Cnz_0 \exp \{-mg(z_c - z_{G_0})/kT\} \quad (47)$$

Where  $z_{G_0}$  is the depth at the center of gravity of the column of depth  $z_0$ . From Eqs. (46) and (47),  $z_0$  can be expressed as:

$$z_0 = \frac{kT/mg [\exp \{-mg(z_c - z_0)/kT\} - \exp \{-mgz_0/kT\}]}{\exp \{-mg(z_c - z_{G_0})/kT\}} \quad (48)$$

For the entire system,  $N_c$ , after integration from  $z=0$  to  $z=z_c$ , can be expressed, as:

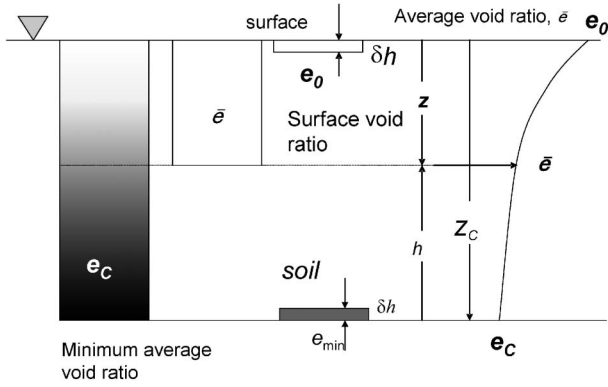


Fig. 8. Interpretation of average void ratio system

$$N_o = Cn(kT/mg)\{1 - \exp(mgz_c/kT)\} \quad (49)$$

and with the average number at the center of gravity,  $z_{Gc}$  as:

$$N_o = Cnz_c \exp\{-mg(z_c - z_{Gc})/kT\} \quad (50)$$

From Eqs. (49) and (50),  $z_c$  is expressed by:

$$z_c = \frac{(kT/mg)\{1 - \exp(mgz_c/kT)\}}{\exp\{-mg(z_c - z_{Gc})/kT\}} \quad (51)$$

b) Relationship between average void ratio and potential energy

Substituting Eqs. (43), (45), (46), (48), (49) and (51) into Eq. (42) gives:

$$\frac{\bar{e}(z) - e_c}{e_o - e_c} = \frac{\exp(-mgz_G/kT) - \exp(-mgz_{Gc}/kT)}{\exp(-mgz_{Go}/kT) - \exp(-mgz_{Gc}/kT)} \quad (52)$$

Since  $z_{Go}$  is close to zero and  $z_{Gc}$  is relatively large, then Eq. (52) can be simplified into the following:

$$\frac{\bar{e}(z) - e_c}{e_o - e_c} = \exp(-mgz_G/kT) \quad (53)$$

$$= \exp(-mgRz/kT) \quad (54)$$

where  $Rz = z_G$  and  $\beta = mgR/kT$ .

Since  $\beta z$  is smaller than 2.0, as derived by  $e = e_{min}$  in Eq. (55), the calculated error between Eqs. (52) and (54) is less than 0.011%.

## DISCUSSION

### Profile of Average Void Ratio

An evaluation of Eq. (54) was performed experimentally by sedimentation tests by Fukue et al. (1987). The procedure is briefly described in later section. The average void ratios were measured on the sediments in water. The results showed that  $\beta (= mgR/kT)$  was almost constant for a bentonite clay sediment profile in sea water as shown in Fig. 10. Therefore, the value of  $mgR/kT$  is almost constant. The true void ratio profile shown in the figure was converted theoretically using the theoretical relationship between average void ratio and true void ra-

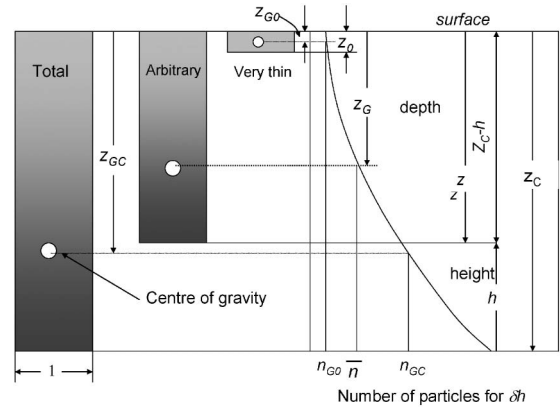


Fig. 9. Potential energy of a particle at the center of gravity

tio (Fukue and Okusa, 1987), which shows that the void ratio decreases rapidly within a depth of 5 cm.

It was noted that the sediments consolidated under very low self-weight and that the particles were usually flocculated. Therefore, the energy system of the sediments would be different from that of the lower, more consolidated sediments. Nevertheless, the derived equations were feasible for expressing the profiles of both the upper and lower sediments (Fukue et al., 1987; Fukue and Okusa, 1987).

### Average Void Ratio - Overburden Pressure Relationship

As mentioned previously, the relationship between the average void ratio and the overburden pressure is expressed by Eq. (2), while the average void ratio is given in Eqs. (53) and (54). Therefore, Eq. (2) provides a state of the soil in terms of potential energy of the particles in it. Equation (53) or Eq. (54) or Eq. (2) is applicable as was shown in Fig. 10.

### Compression Process

The equations theoretically derived from this study were given experimentally in Fukue and Okusa (1987). The average void ratio was mathematically converted to the corresponding true (ordinary) void ratio, using Eq. (3), where the true void ratio is defined as the conventional void ratio of an element at an arbitrary depth. The true void ratio profile is expressed by:

$$\frac{e - e_{min}}{e_o - e_{min}} = 0.119 + 0.881(1 - \beta z) \exp(-\beta z) \quad (55)$$

where  $e$  is the void ratio of an element as a function of  $z$  and  $e_{min}$  is the minimum void ratio of a given element (Fukue and Okusa, 1987). In Eq. (55), if  $e = e_{min}$ ,  $\beta z$  becomes two. This indicates that  $\beta z$  will change from zero to two for any soil system. Equation (55) gives a form of the void ratio profile with depth. To obtain Eq. (55), the following theoretical relationship (Fukue and Okusa, 1987) is used:

$$e_{min} = e_c - 0.135(e_o - e_c) \quad (56)$$

The equations obtained are also applied to describe the

consolidation behaviour of soils. In order to apply Eq. (55) to this behaviour, the  $e_0$  is taken as the initial void ratio of the soil sample. The void ratio-pressure relationship can be obtained using Eqs. (2) and (55) where  $z$  is no longer considered as depth but as a variable to express interparticular energy, as described later. The theoretical  $e$ - $\log p$  relationships obtained from Eqs. (2) and (55) agree with the experimental results shown in Fig. 11. The  $\beta$  value is constant for each loading, unloading and reloading. This indicates from an energy point of view that the soil types are different for each type of loading since the size of the energy system is different as will be described later.

The set of equations suggests that the  $e$ - $\log p$  curve may not overlap at any point if the initial void ratio,  $e_0$  is different. The lower the initial void ratio, the lower the slope which is conventionally expressed as compression index. The empirical relationships between the initial void ratio or initial water content and compression index are well known. This trend is seen in Fig. 11, though the difference between the slopes which result from the different initial void ratios is small.

On the other hand, there is the concept that the soil state will return to the natural, unsampled condition by reloading the sampled soil. This is usually assumed in many engineering applications, testing soil samples, consolidation theory and others. However, it is apparently in contradiction to the above mentioned, i.e., dependency on the initial condition.

Thus, there is the possibility that any sampled soil is different from soils under natural conditions. Although the influence of the stress release by sampling has often been explained from the disturbance of the sample, there may be inherent properties of sampled and natural soils which should be understood as the different soil systems with different initial states.

Figure 12 shows the compression behaviour of Toyoura sand and an oil sand. The data of the oil sand was obtained from Roberts (1964). The lines indicated in the figure are theoretical, by assuming initial and minimum void ratios and  $\beta$  values. The frictional resistance of the oil sand is weaker than ordinary sands, because of the oil between the particles. For ordinary sands, the  $\beta$  value is smaller than that of the oil sand. In fact, the compression behaviour of sands is similar to clayey soils (Coop, 1990), which may imply that there is a universal expression for soil compression.

#### Relative Density of Sand

The state of sand is often expressed by the relative density, which is defined using Eq. (55) and by taking  $e_{\max} = e_0$ , we obtain

$$1 - D_r = \frac{e - e_{\min}}{e_0 - e_{\min}} = 0.119 + 0.881(1 - \beta z) \exp(-\beta z) \quad (57)$$

where  $D_r$  is the relative density of sand, which is a state parameter indicating how dense a given sand sample is. Thus the relative density of sand can be expressed as a function of an energy term  $\beta (= mgR/kT)$  and  $z$ .

Cubrinovski and Ishihara (2002) stated that  $e_{\max} - e_{\min}$  can provide valuable and unique information about the material properties of sandy soils and it can be particularly effective in evaluating the potential of compressibility and contractiveness of cohesionless soils. This probably is dependent on Eq. (57) obtained in this study. Since  $\beta z$ , defined as relative energy or also as normalized energy ranging from 0 to 2.0 as was described earlier, the relationship between  $D_r$  and  $\beta z$  is unique as shown in Fig. 13. The simple concept of relative energy is that  $\beta z = 0$  at the initial state or loosest state, and that  $\beta z = 2.0$  at the final state for a compression process or the densest state in a soil profile system.

Though we assumed that  $e_{\max} = e_0$ , they are not always equal. The  $e_0$  state can be obtained at any time with unloading, which is not  $e_{\max}$  which is the void ratio at the loosest state of sand. Therefore, it is important to know the state of sand in terms of  $D_r$  in Eq. (57), the pressure, and the initial states (void ratio). Thus, the states of sand correlate with an energy state defined in this study. A more detailed examination of the relative density for sand can be possible using Eq. (57).

## CONCEPT OF IMAGINARY PARTICLES

### Soil System and Compression Process

As shown in Figs. 10 to 12, the compression behaviour of soils or the change in soil state under compression is expressed by the equations derived in this study. It is important that in the cases shown in these figures, the compression behaviour or change in state is basically described by the constant  $\beta$ . It is important to realize that Fig. 10 is an application of Eq. (53) for describing a soil profile, i.e., the soil system (Fukue et al., 1987). The figure was an example of many experiments obtained by a long term sedimentation experiment. The average void ratio was obtained by settling the slurry samples 18 times into a one-liter glass cylinder with a certain amount of water. A few grams of the slurry sample were poured into the cylinder and left until the settlement of the deposit was finished. Then the volume of the sediment was measured. The first average void ratio was calculated using the

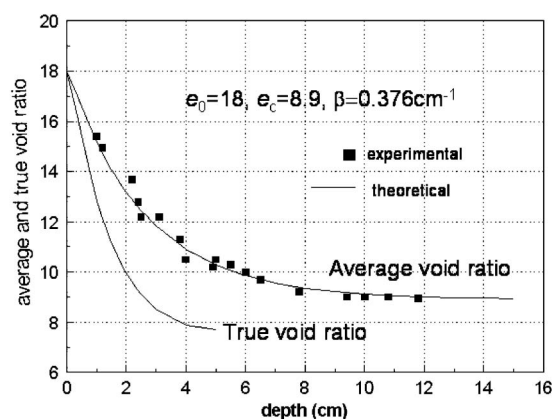


Fig. 10. Average void ratio profile in a sedimentation test

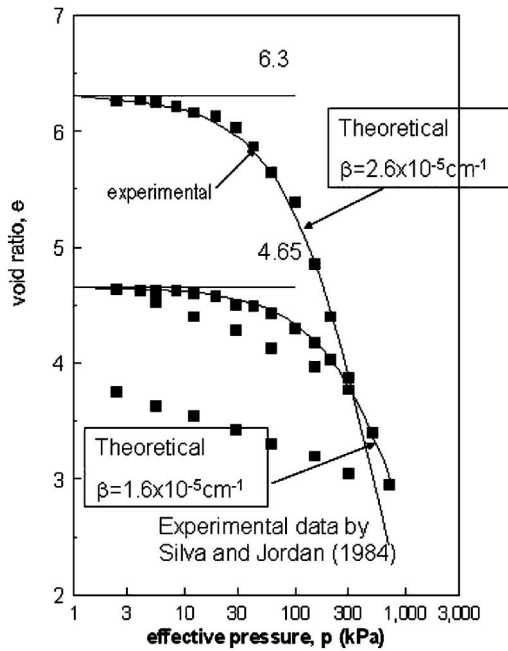


Fig. 11. Compression curves of marine soils, including unloading and reloading processes (data from Silva and Jordan, 1984)

volume and dry weight of the sample poured. Next, a few grams of slurry sample were poured in to the cylinder. After the settlement of the deposits was finished, the average void ratio of the first and second deposits was obtained. These procedures were repeated until the asymptotic average void ratio was obtained, as shown in Fig. 10. Thus the thickness of the deposits increases. The existence of an asymptotic void ratio indicates that the compression apparently stops at a given void ratio, i.e.,  $e_c$  or  $e_{min}$  of this sediment. Thus,  $e_{min}$  is defined as the void ratio where the deformation stops under the present loading stress. In addition, it is a transition point from this loose state to the next stage. The  $\beta$  value was determined for the best fit using the asymptotic void ratio and the assumed surface void ratio. Though the  $\beta$  value has a physical meaning; at present it is used as a parameter that connects the initial void ratio with  $e_{min}$ . It should be noted that the deposit obtained is the top layer of sediment soil, which can be described by a  $\beta$  value of approximately  $0.4 \text{ cm}^{-1}$  for various types of soil samples and natural sediments with different ranges of the average void ratio (Fukue et al., 1987). Thus, a transition at a very loose state can be found at  $z = 0.5 \text{ cm}$ , because  $z = 2.0/0.4$ . This is almost independent of the type of soil.

Figures 11 and 12 show an application for expressing the consolidation behaviour of soil, i.e., the compression process. The initial void ratio,  $e_0$  is not difficult to estimate from the  $e$ - $\log p$  relationships. The  $e_{min}$  is a little difficult to predict, because it is dependent on the geometry of the particles. However, the first trial is to use 0.5 for the  $e_{min}$ . Figure 12 shows that the  $e_{min}$  of oil sand for the best fit is low, because oil can reduce the closest packing void ratio. This  $e_{min}$  provides the transition point to the next compression stage under greater loads. Thus, the

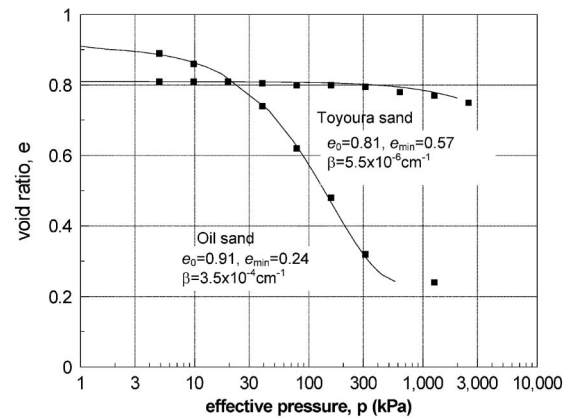


Fig. 12. Compression curves of a Japanese standard sand, and oil sand (data by Roberts, 1964)

equations derived in this study can be applied to describe both the soil system and soil processes. Therefore, it may be possible to compare artificial and natural compression behaviour using the equations.

#### Imaginary Particles

For the derivation of Eq. (53), it was assumed that  $m$  was the mass of a particle and that the potential energy is only dependent on the elevation of the particle. However, this is not the case. It is obvious that the mass  $m$  calculated from the experimental  $\beta$  is not the actual value for the particle, but it includes the effects of interactions between particles.

Therefore, it must be considered that the potential energy defined by  $mgh$  is not only dependent on the elevation of the particle, but also on the interparticle forces acting between the particles or interparticle energy. This is due to the relationship of the interactions with the void ratio profile. This is analogous to the situation of potential energy of a mass suspended on a spring, depending on the elasticity of the spring.

Therefore, in this study the particle which can be imaginatively represented by the experimental  $\beta$  is defined as an "imaginary particle" in any soil system. For example, the different  $\beta$  values for the respective curves, shown in Fig. 11 provide the different sizes of imaginary particles relating to the mass, respectively.

## APPLICATION TO VARIOUS TYPES OF SOILS

### Interactions between Particles

There are many types of interactions between soil particles, which depend upon mineralogy and size distribution of particles, interfacial phenomena between particles and pore liquids and interactions namely, the contact between particles, as known in soil physics, soil chemistry, soil mechanics and geotechnical engineering. The  $\beta$  value will be influenced by these factors and typical examples can be as follows:

- The cementation between particles will lower the  $\beta$  value if the void ratio is the same. The cementation of

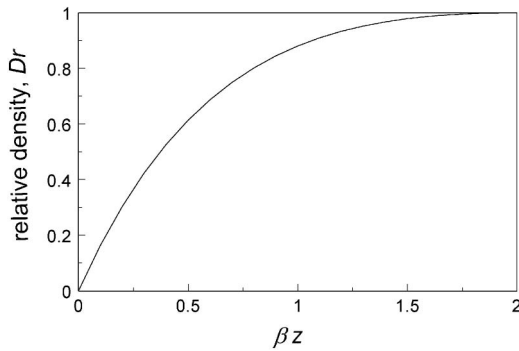


Fig. 13. Relationship between relative density  $D_r$  and  $\beta z$

soils has not been fully understood. It has been explained by factors such as salt for quick clay (Rosenvqvist, 1953), organic matter (Pusch and Arnold, 1969), amorphous materials (glass in volcanic soils), carbonates (Fukue et al., 1999; Fukue and Nakamura, 1996; Imai et al., 2006) and others. If the cementation is relatively strong at higher void ratios, it will be broken down easily during compression and then, the  $\beta$  value will be increased largely. It is noted that an increasing  $\beta$  value means weaker interactions.

- b) The change in the interfacial forces due to the change in properties of pore water will cause the interactions between particles. A good example can be obtained for an active clay- electrolyte system. For example, the mechanical properties of bentonite clay will be drastically changed by adding salt. Therefore, if the electrolyte solution is allowed to penetrate into the soil, then the interactions are weakened (Fukue et al., 1986). Consequently, the  $\beta$  value will increase.
- c) For the case of a sand-clay mixture, the mechanical properties of the soil are dependent on the fabric. If there is no significant contact between sand fractions, the soil may behave like a clay soil. However, if the contacts between sand fractions will be formed during the consolidation of clay fractions, the soil is more likely a sand with cohesion (Fukue et al., 1986). These provide a change in the  $\beta$  value. The development of frictional resistance due to the formation of contacts between sand fractions will decrease the  $\beta$  value.

Since the relationship between undrained shear strength,  $s_u$  and effective stress,  $p$  is often expressed as  $s_u/p = \tan \phi$  ( $= \text{constant}$ ), the  $e$ - $\log p$  curve becomes parallel to the  $e$ - $\log s_u$  curve, when  $p$  and  $s_u$  are plotted using the same axis. The  $\phi$  is defined as the angle of undrained shearing resistance. Thus, the  $\beta$  value can also be correlated to the undrained shear strength. The details of this will be shown in another paper under preparation.

#### Change in the Energy System during Compression

The change in the energy system will affect the change in partition function,  $P$  and  $m$ , resulting from the change in the type of interactions between particles. However, in the fundamental equation, Eq. (35), the  $P$  has been eliminated. Therefore, the change in the energy system will in-

fluence the value of  $m$ , as well as the void ratios, such as  $e_o$  and  $e_{min}$ .

Actual compression curves for an undisturbed soil sample can be demonstrated in Fig. 14. The data plotted are typical examples of Mexico City clays, obtained by Zeevaert (1957). Other data obtained by him and for cemented or sensitive clays obtained by many other researchers show similar trends (Mesri et al., 1975; LaRochelle et al., 1980; Burland, 1990). The experimental data show that the compression for undisturbed sample breaks the bonds between particles, consequently causing a disturbance during compression. This phenomenon is strain softening. Strain softening is, therefore, expressed by an increasing  $\beta$  value. If the sample is initially disturbed, the original compression curve may have a greater  $\beta$  value in comparison to an undisturbed sample. This means that the compression index,  $C_c$  will decrease with the degree of disturbance, as used to evaluate sample quality. It is important to note that actual compression curves exist between the two standard curves for remolded (non-bonded) and undisturbed samples without strain softening. Both lines are similar to the ICL and SCL defined by Burland (1990). The increasing  $C_c$  is due to the strain softening which may be dependent on the initial void ratio and cementation degree.

A big question arises here as to whether or not the breaking of bonds between particles will occur, and how much loading rate is required for that to occur in the field. Because natural compression of sediments under newly deposited particles may not cause the breaking of bonds, it cannot always be assumed that the laboratory test can predict field performance. Only a relatively high loading rate will cause strain softening to occur due to micro-fractures (breaking of bonds) which may not be always achievable in the field. If so, then it is doubtful that it is beneficial to use the experimental  $C_c$  values for prediction of settlement in the field.

Thus, with constant initial and minimum void ratios and different values of  $\beta$ , the compression curves based on the characteristics of the equations, Eqs. (2), (53) and (55), are all parallel. An example is demonstrated in Fig. 15 which shows compression curves with a constant  $\beta$ , i.e.,  $\beta_1$  and  $\beta_2$ , indicated by the solid lines, and also compression curves with a variable  $\beta$  changing from  $\beta_1$  to  $\beta_2$ , indicated by the broken lines, where  $\beta_1 > \beta_2$ . The curve with the variable  $\beta$  changing from  $\beta_2$  to  $\beta_1$  is also feasible.

#### TRANSITION FROM ONE STATE TO ANOTHER

There is no doubt that there may be a transition in the state from soil to rock. This is because the interaction between particles is quite different for both materials. Similarly, there may be no doubt that the suspended solids system, (i.e., the dispersed particles system in water) is different from the sediments deposited in water. The readers may think that suspended solids are not soils. However, we may think that sediments are also suspended and settling while interacting. In fact, the settling ve-

locity of sediments can be measured and there is no consolidation due to the excess pore water pressure. Therefore, the difference between suspended solids and sediments results from the different interactions for both materials. In the dispersed system, the repulsions between the particles overcome the attractions. On the other hand, settled particles may be aggregated with no dominant repulsive forces between the particles.

Marine soils often have a higher water content than the liquid limit. In general, the top 1 or 2 m of the sediment layers have a water content higher than the liquid limit. These soils have very loose but relatively firm structures. These soils will be easily collapsed even under a laterally confined condition. Therefore, the deformation properties above and below the liquid limit may be different. Thus, if the deformation properties will change, there may be a transition during compression. In this study, the possible transitions can be found using the equations derived with the experimental results.

#### *Transition at the Liquid Limit*

In the process of natural consolidation, there are some transitions from one form to another. For example, clay and shale can be cited as a transition from soil to rock. Other transitions can exist in suspended systems and deposited surface sediments. These transitions can be described as the change in the type of interparticle energy from one to another. The simplest example is the transition from uncemented sand to sandstone.

In the case of sediments, they usually have a structure of floc-like aggregates. The pressure to the self weight counteracts the pressure between the flocs. The compression and/or consolidation first occurs without collapsing the flocs under a very low overburden pressure. The macro-pores formed by flocs will then collapse under their own weight during the sedimentation of new flocs. Once this has occurred, the interparticle interactions become dominant. Therefore, there must be a transition occurring in this case.

The liquid limit of soil is also an example of a transition, which can be defined as a transition from liquid to plastic states. To examine this, a consolidation test on a commercially available clay using centrifugal force was performed at Kyoto University. The test specimen of  $10.2 \times 50 \times 16.8$  cm ( $W \times L \times H$ ) was consolidated for 17 hours in which no deformation was observed, under a gravity of 20 g. The soil sample had an initial water content of 65% (liquid limit; 43% and plastic limit; 23%). The arm length of the centrifuge was 2.5 m. Water content was measured on the sliced sample from the consolidated specimen. The experimental results are shown in Fig. 16 along with the theoretical relationships obtained in this study. From the experimental results, two sets of constant parameters,  $e_0$ ,  $e_{min}$  and  $\beta$  are determined. Between the two curves using the two sets of parameters, the transition is clearly seen near a void ratio ( $= 1.17$ ) at the liquid limit of the supplemental (theoretical) curves for soils having a water content higher and lower than the liquid limit. Since the sample used was initially homogene-

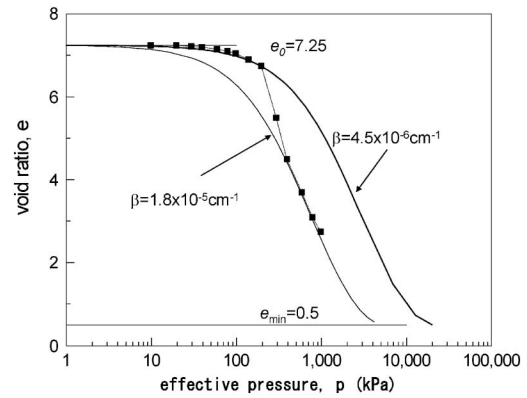


Fig. 14. The  $e$ -log  $p$  curves for a strongly cemented, volcanic soil in Mexico City (data from Zeevaert, 1957)

ous, there was little scattering for this consolidation result. Thus, the transition obtained at the liquid limit is likely to be real. It is emphasized that without theoretical curves, the experimental result cannot be properly understood and would only be a collection of empirical data.

#### *Transition at a Low Void Ratio and High Pressure*

An example of the transition of marine sediments is shown in Fig. 17. The data were obtained from the marine deposited soil of North Hokkaido (Aoyagi, 1978). The lines indicated in Fig. 17 express ordinary soils obtained using the values,  $e_0 = 4$ ,  $e_{min} = 0.5$  and  $\beta = 1.5 \times 10^{-5} \text{ cm}^{-1}$  for the shallower sediments and  $e_0 = 0.5$ ,  $e_{min} = 0$  and  $\beta = 1.7 \times 10^{-6}$  for the deeper sediments which can be classified as sedimentary rocks. The theoretical curve was determined as the best fit using these constant parameters,  $e_0$ ,  $e_{min}$  and  $\beta$ . If any of these is not properly determined, the theoretical line will deviate entirely from the experimental points. This apparently shows that a void ratio of 0.5 is almost the densest packing state for particulate materials in nature, and that compression beyond this void ratio leads to the deformation or creep of particles (Fukue and Okusa, 1987). With the theoretical relationships, the transition between them is apparent, which is similar to Fig. 16. The deviation of the data from the computed line may be due to the varied nature of sediments with respect to grain size, mineralogy and other constituents, because of the considerable interval of depth.

Since compression of soil may stop at once at the closest packing state of constituents, where no more sliding between particles occurs, continuous compression may provide a significant creep deformation of particles themselves, i.e., formation of the next stage of sediment. Aoyagi (1978) mentioned that in the compression of montmorillonite clay, there is a transitional state at a porosity of 30%, which is close to the  $e_{min}$  for this stage. Thus, the  $e_{min}$  is the void ratio where the deformation will stop immediately during continuous compression loading. This will occur when the type of interactions and structure will change, as was shown in this study.

In Fig. 17, the maximum depth of the shallower sedi-

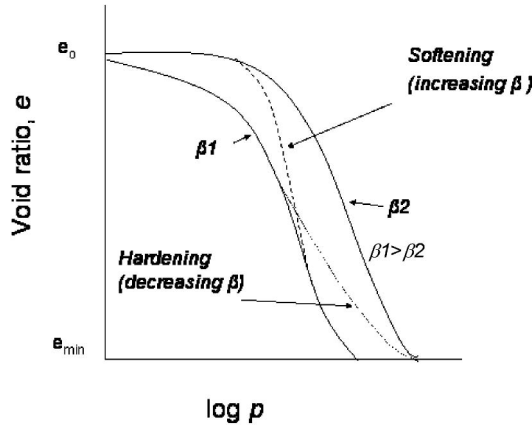


Fig. 15. Compression curves with variable  $\beta$  values in relation to strain softening and hardening

ments is approximately 1330 m. The effective pressure calculated from Eq. (2) at the maximum depth is approximately 9200 kPa. The  $e_{min}$  for the shallower sediments is defined as the initial void ratio of the next deeper sediments.

The soil states related to the stages can be demonstrated in Fig. 18. The zero order stage shown in Fig. 18(a) can be identified as the dispersed particles in water. The particles are suspended due to the relatively strong repulsion. For example, this stage is found as suspended bentonite clay particles dispersed in distilled water. Basically, this stage does not exist for sand. Figure 18(b) illustrates the most top layer under water, when the flocculated structure with macro pores. This layer is identified as a drifting layer at the first stage, with a thickness of about 5 cm (Fukue et al., 1987). The macro-pores disappear when the average void ratio reaches  $e_c$ , where the soil state is transformed into the next stage, i.e., the second stage, as shown in Fig. 18(c). A soil in this stage has a water content higher than the liquid limit. It is noted that this type of soils usually have a thickness, about a few meters in marine conditions. Since the water content for this type of soil is higher than the liquid limit,  $w_L$ , it becomes liquid like easily by disturbance. The ordinary soils can be defined as the soil with a water content lower than the liquid limit, as shown in Fig. 18(d). This type of soil is mostly encountered in engineering practice. The following compression process, i.e., diagenesis for a long time, will produce the sedimentary rock. This stage can be illustrated in Fig. 18(f). As was shown through this study, the equations derived can be applied to express the compression behaviour of these types of soils shown in Fig. 18. The  $\beta$  and  $\beta z$  to be determined can be used to characterize the soil state.

**COMPRESSION INDEX**

The compression index is defined as the slope of the linear portion of  $e$ - $\log p$  curve and is used for estimating the settlement of ground. If we define the slope of  $e$ - $\log p$  relationship by  $de/d \log p$ , we obtain the following

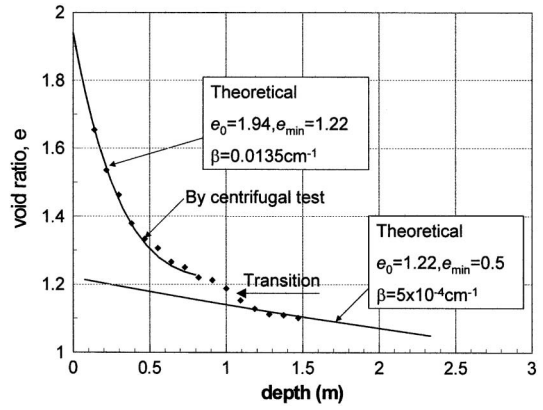


Fig. 16. Results of the change in void ratio of a commercially available clay during a centrifugal consolidation test

relationship (Fukue and Okusa, 1987),

$$C'_c = \frac{de}{d \log p} = \frac{2.3(2-E)E(e_0 - e_c) \{1 + e_c + (e_0 - e_c)A\}A}{1 + e_c + (e_0 - e_c)(1 + E)A} \quad (58)$$

where,  $A = \exp(-E)$ ,  $E = \beta z$ . The following theoretical relationship can then be used,

$$e_c = \frac{e_{min} + 0.135e_0}{1.135} \quad (59)$$

Therefore, the compression index can be defined as the maximum of the  $C'_c$  value. Strictly speaking, the maximum value of  $C'_c$  is a little greater than the compression index, because the conventional compression index is the maximum slope of the assumed straight portion of  $e$ - $\log p$  curve, but the maximum value by Eq. (58) is taken as the tangent to the nonlinear relationship. In fact, it is noted that there are no linear portions for the  $e$ - $\log p$  relationships for soils (Fukue and Okusa, 1987). Since the maximum value of  $C'_c$  is given at approximately  $E = 0.5$  (Fukue and Okusa, 1987), then Eq. (58) can be expressed by substituting Eq. (59) as

$$C_c = - \frac{0.926(e_0 - e_{min}) \{1 + 0.653e_0 + 0.347e_{min}\}}{1 + 0.921e_0 + 0.079e_{min}} \quad (60)$$

Thus,  $C_c$  is expressed in terms of  $e_0$ , which may not largely differ from those obtained by many researchers, as summarized by Yoon et al. (2004) and Giasi et al. (2003). The difference between Eq. (60) and empirical relationships is their degree of linearity. Although most empirical relationships are linear, there is usually no theoretical basis for this and there is always some scattering of the data.

When soils are saturated, the initial void ratio,  $e_0$  can easily be converted into water content,  $w$ , as,

$$w = e_0 / G_s \times 100\% \quad (61)$$

where  $G_s$  is the specific gravity of particles. Substituting this into Eq. (60), the following is obtained,

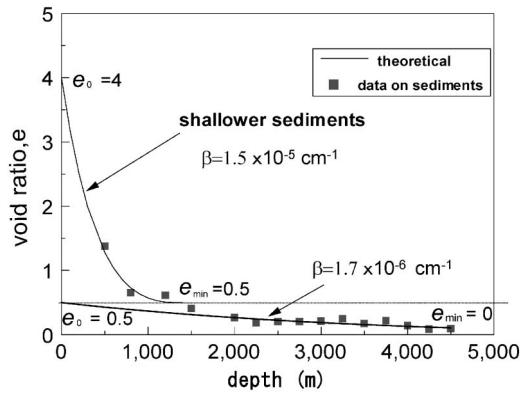


Fig. 17. Void ratio profiles of deep sediments (Aoyagi, 1978), and theoretical relationships showing the transition between them

$$C_c = \frac{0.926(wG_s/100 - e_{min})(1 + 0.653wG_s/100 + 0.347e_{min})}{1 + 0.921wG_s/100 + 0.079e_{min}} \quad (62)$$

Taking soil systems which can be expressed by an  $e_{min}$  of 0.5, the relationship between  $C_c$  and  $w$  can be obtained. It is noted that the assumption of the  $e_{min}$  provides for soils existing in the normal soil stage. Herein it is noted that the  $e_{min}$  is defined as the void ratio which provides a  $C_c$  value of zero. Therefore, it can be regarded as the closest packing state of soil particles under a stress range.

Figure 19 shows the values of  $C_c$  for various soil samples and empirical relationships (after Mesri and Rokhsar, 1974) and the theoretical relationship using Eq. (62). For the theoretical relationship, the value of  $G_s$  was assumed to be 2.65. It can be seen that the theoretical relationship agrees well with the empirical relations and shows the relations for various soils. Figure 19 implies

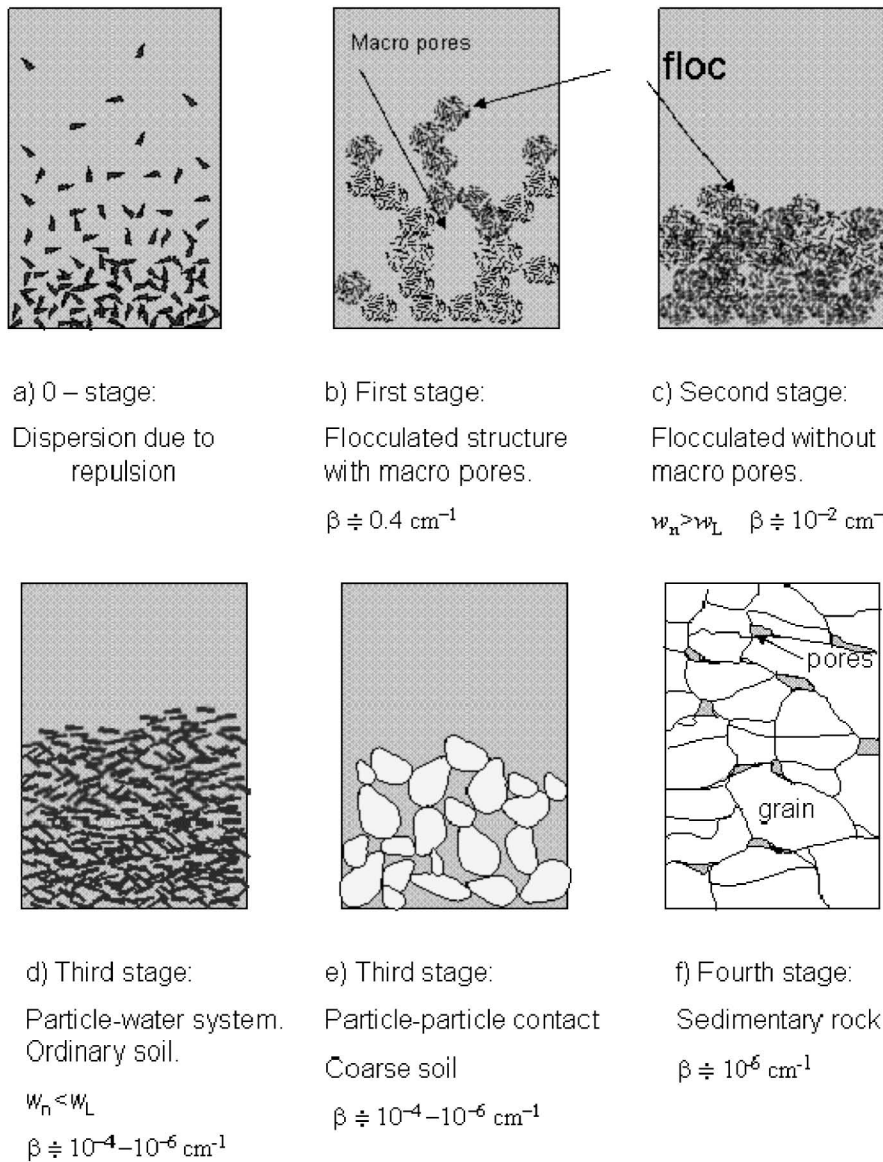


Fig. 18. Illustration of various soil systems and types of interactions with approximate  $\beta$  values.  $w_n$ : natural water content,  $w_L$ : liquid limit

1. Amorphous and fibrous peat
2. Calcareous organic silt
3. Soft to medium clay
4. Mexico City clay
5. Victoria marine clay
6. Organic silty clay
7. Peaty organic silt
8. Canadian muskeg
9. Kingston Marsh deposit
10. Soft varved clay
11. Strified silty clay and sand
12. Bangkok marine clay
13. Whangamarino clay
14. Marine silty clay
15. Sensitive marine clay
16. Rutherford clay

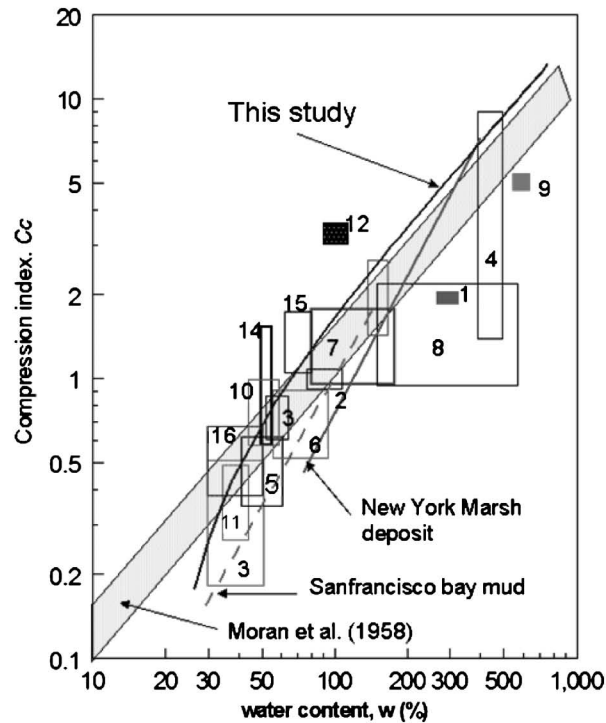


Fig. 19. Theoretical and empirical relationships for compression index as a function of initial water content. The empirical relationships are adapted from Mesri and Roksar (1974)

that many kinds of marine clays and sensitive clays have higher  $C_c$  values than the theoretical ones. This is because of strain softening during compression, as shown in Fig. 14. Canadian muskeg has a lower  $C_c$  than the theoretical one. This may be the result of organic fragments as constituents and structural characteristics, such as  $e_{min}$ . If the  $e_{min}$  is greater than 0.5, the theoretical  $C_c$  is lower. The deviation may be due to behaviour including strain softening and the effect of sand content during compression (Fukue and Okusa, 1985). If the sand content is relatively high, frictional resistance will be developed during volume change. Accordingly, it is likely then that  $C_c$  will tend to lower to the corresponding initial void ratio of the sand.

There are many empirical relationships between the compression index and Atterberg limits, as summarized by Giasi et al. (2003). These include the assumption that the natural water content is higher for fine soils with a higher liquid limit. However, there is no theoretical basis for the compression index to be based on liquid limits. In this study, it has been shown that there is basis for the relationship of compression index with the initial and minimum void ratios.

## CONCLUSIONS

Difficulties in soil mechanics exist since there is no "equations of state for soil." This is because soil is a highly compressible and irreversible material with interactions between the constituents. Since a state of soil should be expressed in terms of void ratio, pressure and energy terms, the equations proposed will make it easy to

deal with soils in a more scientific manner. In this manner, some misunderstandings such as regarding compression behaviour of soils can be eliminated. This theoretical approach was successfully applied to a wide variety of situations and soils.

In summary, the following conclusions can be made:

- a) There is a universal relationship for volume and effective pressure, which is derived using statistical mechanics.
- b) The general compression curve for soils can be determined by initial and final (minimum) void ratios and a constant  $\beta$  value which is related to the potential energy of a soil element.
- c) The general relationships and experimental results imply that different soil systems in nature, such as suspended, deposited (flocculated), liquid-like (water content higher than the liquid limit), consolidated (ordinary soils) and strongly cemented soils (rock), can be distinguished from each other by their transition behaviour. Different soil systems have been expressed by the corresponding parameters, i.e.,  $e_0$ ,  $e_{min}$ , and  $\beta$  values.
- d) The standard compression index (without strain softening or hardening) is only dependent on the initial and final (minimum) void ratios. The initial cementation magnitude will provide the  $\beta$  value.
- e) Strain softening and hardening during compression will lead to a change in the  $\beta$  value.
- f) Thus, consolidation behaviour can be quantitatively analyzed in detail using this constant and its change.
- g) Compression index is a primary function of  $e_0$  and  $e_{min}$ , whereas strain hardening and softening are sec-

- ondary factors. The classification of the soil according to the liquid limit may be affected by the water content (void ratio) at sedimentation, which may then appear that the Atterberg limit influences the  $C_c$ .
- h) The developed formula can be applied for various soils including sand.
  - i) From the formula, it is shown that the relative density of sand has a physical meaning.
  - j) Through this study, it is concluded that the developed formula constitutes the state equation for soils.

## ACKNOWLEDGEMENTS

The centrifugal consolidation test was performed by Dr. K. Kita, Tokai University, at the Disaster Prevention Research Institute, Kyoto University. The authors thank Dr. K. Kita and Prof. M. Kamon, Kyoto University, for their cooperation. Special thanks are given to the late Prof. G. Imai for his encouragement throughout this study.

## REFERENCES

- 1) Aoyagi, K. (1978): Diagenesis of marine argillaceous sediments, *The Memoirs of the Geological Society of Japan*, **15**, 3–14 (in Japanese).
- 2) Been, K. and Sills, G. C. (1981): Self-weight consolidation of soft soils: an experimental and theoretical study, *Géotechnique*, **31**(4), 519–535.
- 3) Burland, J. B. (1990): On the compressibility and shear strength of natural clays, *Géotechnique*, **40**(3), 329–347.
- 4) Butterfield, R. (1979): A natural compression law for soils, *Géotechnique*, **29**(4), 469–480.
- 5) Coop, M. R. (1990): The mechanics of uncemented carbonate sands, *Géotechnique*, **40**(4), 607–626.
- 6) Cubrinovski, M. and Ishihara, K. (2002): Maximum and minimum void ratio characteristics of sands, *Soils and Foundations*, **42**(6), 65–78.
- 7) Fukue, M., Okusa, S. and Nakamura, T. (1986): Consolidation of sand-clay mixtures, *Consolidation of Soils*, ASTM, **STP 892**, 627–641.
- 8) Fukue, M. and Okusa, S. (1987): Compression law of soils, *Soils and Foundations*, **27**, 23–34.
- 9) Fukue, M., Yoshimoto, N. and Okusa, S. (1987): General characteristics of upper soil sediments, *Marine Geotechnology*, **7**, 15–36.
- 10) Fukue, M. and Nakamura, T. (1996): Effects of carbonate on cementation of marine soils, *Marine Georesources and Geotechnology*, **14**, 37–45.
- 11) Fukue, M., Nakamura, T. and Kato, Y. (1999): Cementation of soils due to calcium carbonate, *Soils and Foundations*, **39**(6), 55–64.
- 12) Giasi, C. I., Cherubini, C. and Paccapelo, F. (2003): Evaluation of compression index of remoulded clays by means of Atterberg limits, *Bull. Engineering Geology. Env.*, **62**, 333–340.
- 13) Imai, G. (1980): Settling behaviour of clay suspensions, *Soils and Foundations*, **20**(2), 61–77.
- 14) Imai, G. (1981): Experimental studies on sedimentation mechanism and sediment formation of clay materials, *Soils and Foundations*, **21**(1), 7–20.
- 15) Imai, G., Komatsu, Y. and Fukue, M. (2006): Consolidation yield stress of Osaka-Bay Pleistocene clay with reference to calcium carbonate content, *ASTM, STP 1482*, 89–97.
- 16) LaRochelle, P., Sarrailh, J., Tavenas, F., Roy, M. and Leroueil, S. (1980): Causes of sampling disturbance and design of a new sampler for sensitive soils, *Can. Geotech. J.*, **18**(1), 52–66.
- 17) Leroueil, S. and Vaughan, P. R. (1990): The general and congruent effects of structure in natural soils and weak rocks, *Géotechnique*, **40**(3), 467–488.
- 18) Mesri, G. and Rokhsar, A. (1974): Theory of consolidation for clay, *J. Geotechnical Engineering Division.*, ASCE, **100** (GT8), 889–904.
- 19) Mesri, G., Rokhsar, A. and Bohor, B. F. (1975): Composition and compressibility of typical samples of Mexico City clay, *Géotechnique*, **25**(3), 507–554.
- 20) Moran, D. E. et al. (1958): Study of deep soil stabilization by vertical sand drains, *OTS Report*, DB151692, Bureau of Yards and Docks, Dept. of the Navy, Washington DC.
- 21) Nishida, Y. (1959): A brief note on compression index of soil, *J. Soil Mechanics and Foundation Div.*, ASCE, **82**(SM3), 1–14.
- 22) Oswald, R. H. (1980): Universal compression index equation, *J. Geotechnical Engrg. Div.*, ASCE, **106**, 1179–1199.
- 23) Park, J. H. and Koumoto, T. (2004): New compression index equation, *Journal of Geotechnical and Geoenvironmental Engineering*, ASCE, **130**, 223–226.
- 24) Pusch, R. and Arnold, M. (1969): The sensitivity of artificially sedimented organic-free Illitic clay, *Engineering Geology*, **3**(2), 135–145.
- 25) Reif, F. (1965): *Fundamentals of Statistical and Thermal Physics*, McGraw-Hill, New York, 211p.
- 26) Roberts, J. E. (1964): Sand compression as a factor in oil field subsidence. *Sc.D. Thesis*, Dept. Civil Engineering, MIT, Boston, MA.
- 27) Rosenqvist, J. Th. (1953): Considerations on the sensitivity of Norwegian quick clays, *Géotechnique*, **III**(5), 195–200.
- 28) Schofield, A. N. and Wroth, C. P. (1968): *Critical State Soil Mechanics*, McGraw Hill.
- 29) Silva, A. J. and Jordan, S. A. (1984): Consolidation properties and stress history of some deep sea sediments, *Seabed Mechanics, Int. UTAM*. (ed. by B. Denness), Graham & Trotman, 25–39.
- 30) Skempton, A. W. (1944): Notes on the compressibility of clays, *Quarterly Journal of the Geological Society of London*, **C**(Parts a and 2), 119–135.
- 31) Tolman, R. C. (1979): *The Principles of Statistical Mechanics*, Dover Publications, Inc. New York, 660p.
- 32) Tsuchida, T. (2001): General interpretation on natural void ratio-overburden pressure relationship of marine deposits, *Soils and Foundations*, **41**(1), 127–143 (in Japanese).
- 33) Yoon, G. L., Kim, B. T. and Jean, S. S. (2004): Empirical correlations of compression index for marine clay from regression analysis, *Can. Geotech. J.*, **41**, 1213–1221.
- 34) Zeevaert, L. (1957): Foundation design and behaviour of Tower Latino America in Mexico City, *Géotechnique*, **7**, 115–133.